Excessive endosomal TLR signaling causes inflammatory disease in mice with defective SMCR8-WDR41-C9ORF72 complex function

William McAlpine[a], Lei Sun[a], Kuan-wen Wang[a], Aijie Liu[a], Ruchi Jain[b], Miguel San Miguel[b], Jianhui Wang[a], Zhao Zhang[a], Braden Hayse[a], Sarah Grace McAlpine[a], Jin Huk Choi[a], Xue Zhong[a], Sara Ludwig[a], Jamie Russell[a], Xiaoming Zhan[a], Mihwa Choi[a], Xiaohong Li[a], Miao Tang[a], Eva Marie Y. Moresco[a], Bruce Beutler[a,1], and Emre Turer[a,b,1]

[a]Center for the Genetics of Host Defense, University of Texas Southwestern Medical Center, Dallas, TX 75390-8505; and [b]Division of Gastroenterology, Department of Internal Medicine, University of Texas Southwestern Medical Center, Dallas, TX 75390-8505

Contributed by Bruce Beutler, October 11, 2018 (sent for review August 27, 2018; reviewed by Tomas Ganz and Mitchell Kronenberg)

The SMCR8-WDR41-C9ORF72 complex is a regulator of autophagy and lysosomal function. Autoimmunity and inflammatory disease have been ascribed to loss-of-function mutations of *Smcr8* or *C9orf72* in mice. In humans, autoimmunity has been reported to precede amyotrophic lateral sclerosis caused by mutations of *C9ORF72*. However, the cellular and molecular mechanisms underlying autoimmunity and inflammation caused by C9ORF72 or SMCR8 deficiencies remain unknown. Here, we show that splenomegaly, lymphadenopathy, and activated circulating T cells observed in *Smcr8*$^{-/-}$ mice were rescued by triple knockout of the endosomal Toll-like receptors (TLRs) TLR3, TLR7, and TLR9. Myeloid cells from *Smcr8*$^{-/-}$ mice produced excessive inflammatory cytokines in response to endocytosed TLR3, TLR7, or TLR9 ligands administered in the growth medium and in response to TLR2 or TLR4 ligands internalized by phagocytosis. These defects likely stem from prolonged TLR signaling caused by accumulation of LysoTracker-positive vesicles and by delayed phagosome maturation, both of which were observed in *Smcr8*$^{-/-}$ macrophages. *Smcr8*$^{-/-}$ mice also showed elevated susceptibility to dextran sodium sulfate-induced colitis, which was not associated with increased TLR3, TLR7, or TLR9 signaling. Deficiency of WDR41 phenocopied loss of SMCR8. Our findings provide evidence that excessive endosomal TLR signaling resulting from prolonged ligand–receptor contact causes inflammatory disease in SMCR8-deficient mice.

inflammatory bowel disease | Toll-like receptor | vesicle trafficking | inflammation

The lysosome is a dynamic organelle that serves as the degradative endpoint for endocytosis, phagocytosis, and autophagy. Recently, the SMCR8-WDR41-C9ORF72 (SWC) tripartite complex has been implicated as an important regulator of membrane trafficking pathways that converge on the lysosome (1–8). Two members of this complex, SMCR8 and C9ORF72, contain DENN domains (9, 10), which are commonly found in proteins that act as guanine nucleotide exchange factors (GEF) for specific Rab GTPases, molecular switches that govern membrane traffic within eukaryotes. Indeed, the SWC complex has been shown to provide GEF activity for RAB8A and RAB39B (3, 8) and to interact with a multitude of other Rabs (3, 6–8). A role for the SWC complex in autophagy (2–6) and endocytic transport (7) has been established by studies documenting defects in these processes in the absence of a single complex component. However, the precise function of the SWC complex or its individual members remains poorly defined.

Hexanucleotide repeat expansions in *C9ORF72* are the most common genetic cause of amyotrophic lateral sclerosis and frontotemporal dementia (ALS/FTD) in humans (11). Numerous epidemiologic studies have also documented an increased prevalence of autoimmune diseases in patients with ALS/FTD with or without C9ORF72 mutations, leading to the proposal that these diseases are linked to the same immunological mechanism(s) (12–15). Studies in mice support a causal role for SWC complex dysfunction in autoimmunity. Several groups have reported that loss of C9ORF72 function leads to autoimmunity characterized by enlarged peripheral immune organs, elevated proinflammatory cytokines, and autoantibody production (1, 2, 16, 17). More recently, splenomegaly, lymphadenopathy, and increased autoantibody production in *Smcr8*$^{-/-}$ mice were reported (18), recapitulating the central phenotypes observed in *C9orf72*$^{-/-}$ mice. Macrophages derived from *C9orf72*$^{-/-}$ mice exhibit increased lysosomal number and exaggerated responses to the proinflammatory stimuli peptidoglycan CpG and silica (1). *C9orf72*$^{-/-}$ mice exhibited elevated splenic levels of LC3, P62, and LAMP1 supporting an in vivo role for the protein in regulation of autophagy (1, 2). The primary cause of spontaneous inflammation in *C9orf72*$^{-/-}$ and *Smcr8*$^{-/-}$ mice has not been identified, but altered autophagy (1, 2, 17) and elevated lysosomal exocytosis (18) have been proposed as potential mechanisms.

Significance

Activation of Toll-like receptors by microbes or host-derived molecules triggers signaling that promotes inflammation and may contribute to the development of autoimmunity. Here we show that excessive signaling by the innate immune Toll-like receptors (TLRs) TLR3, TLR7, and TLR9 is causative for inflammatory disease in mice with mutations of *Smcr8*. The cellular mechanism for their hyperactivation is likely prolonged ligand–receptor contact in lysosomes and phagosomes, the trafficking of which is regulated by the SMCR8-WDR41-C9ORF72 complex in immune cells. We also show that *Smcr8* and *Wdr41* mutations sensitize mice to chemically induced colitis. Our findings reveal an important negative regulatory mechanism that limits endosomal TLR signaling and shed light on the mechanism by which deficiencies of C9ORF72 or SMCR8 cause inflammation.

Author contributions: W.M., B.B., and E.T. designed research; W.M., L.S., K.-w.W., A.L., R.J., M.S.M., J.W., Z.Z., B.H., S.G.M., J.H.C., and X. Zhong performed research; S.L., J.R., X. Zhan, M.C., X.L., and M.T. contributed new reagents/analytic tools; W.M., B.B., and E.T. analyzed data; and W.M., E.M.Y.M., B.B., and E.T. wrote the paper.

Reviewers: T.G., University of California, Los Angeles; and M.K., La Jolla Institute for Allergy and Immunology.

The authors declare no conflict of interest.

[1]To whom correspondence may be addressed. Email: bruce.beutler@utsouthwestern.edu or emre.turer@utsouthwestern.edu.

This article contains supporting information online at www.pnas.org/lookup/suppl/doi:10.1073/pnas.1814753115/-/DCSupplemental.

Published online November 15, 2018.

Here, we show that loss of SMCR8 or WDR41 function leads to exaggerated signaling from the Toll-like receptors (TLRs) TLR3, TLR7, and TLR9, innate immune receptors sensitive to nucleic acids, the function of which is restricted to endolysosomal compartments. These TLRs are normally trafficked to endosomes, where their activity depends on cleavage by peptidases activated within the acidic environment of the endolysosome (19). TLR3, TLR7, and TLR9 encounter their ligands within the endolysosome and initiate signaling leading to induction of proinflammatory cytokines, type I IFN, and other genes necessary for the innate immune response (19). Our findings suggest that this response is aberrantly activated in SMCR8-deficient mice due to defective lysosome and phagosome maturation, resulting in protracted TLR stimulation and leading to inflammatory disease.

Results

SMCR8 Negatively Regulates Endosomal TLR Signaling. To identify genes involved in the regulation of TLR signaling, we carried out a forward genetic screen in which peritoneal macrophages harvested from third-generation (G3) mice carrying *N*-ethyl-*N*-nitrosourea (ENU)-induced mutations were assayed for TNF secretion after stimulation with TLR ligands in the culture medium. Using superpedigree analysis, a method that evaluates

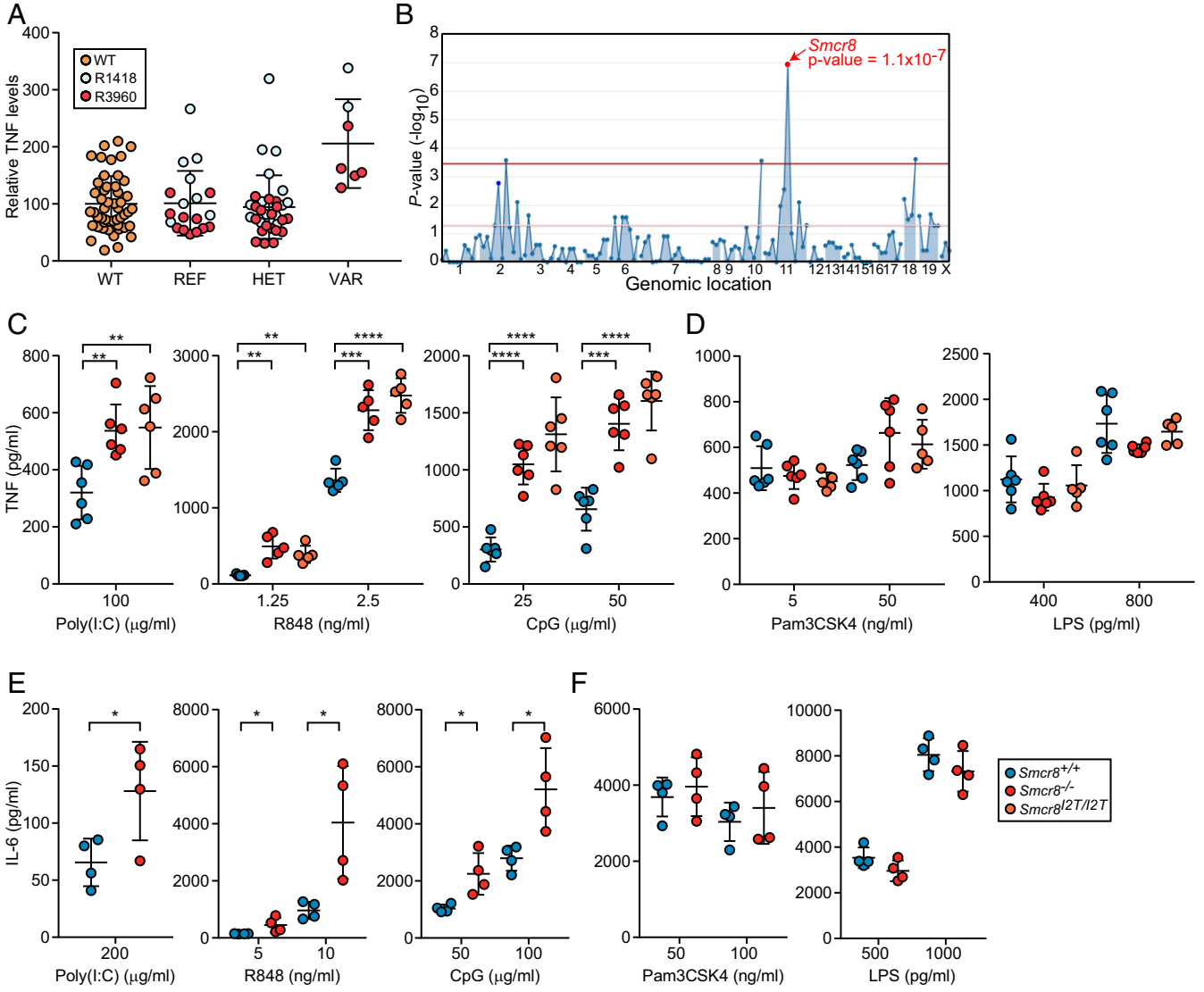

Fig. 1. Analysis of TLR signaling in *Smcr8*$^{-/-}$ and *Smcr8*$^{I2T/I2T}$ myeloid cells. (*A*) Peritoneal macrophages harvested from pedigrees R1418 [REF, *Smcr8*$^{+/+}$ ($n = 8$); HET, *Smcr8*$^{+/p}$ ($n = 15$); VAR, *Smcr8*$^{p/p}$ ($n = 2$)] and R3960 [REF, *Smcr8*$^{+/+}$ ($n = 11$); HET, *Smcr8*$^{+/p2}$ ($n = 18$); VAR, *Smcr8*$^{p2/p2}$ ($n = 5$)] were stimulated with 25 μg/mL of CpG. TNF in the culture medium as measured by ELISA 4 h later. (*B*) Manhattan plot showing *P* values of association between the phenotype of elevated TNF production in response to CpG and mutations identified in the two pedigrees in *A* calculated using a recessive model of inheritance. The $-\log_{10} P$ values are plotted versus the chromosomal positions of mutations. Horizontal red and purple lines represent thresholds of $P = 0.05$ with or without Bonferroni correction, respectively. The *P* value for linkage of *Smcr8* mutations with the elevated TNF production is indicated. (*C* and *D*) ELISA analysis of TNF secretion by peritoneal macrophages ($n = 5$ or 6 mice per genotype) stimulated for 6 h with indicated concentrations of endosomal TLR ligands poly(I:C), R848, and CpG (*C*) or surface TLR ligands Pam3CSK4 and LPS (*D*). (*E* and *F*) ELISA analysis of IL-6 secretion by BMDCs ($n = 4$ mice per genotype) stimulated for 6 h with indicated concentrations of poly(I:C), R848, and CpG (*E*) or Pam3CSK4 and LPS (*F*). In *A* and *C*–*F*, data points represent individual mice. Data are representative of one (*A* and *B*) or three independent experiments (*C*–*F*). Data are expressed as means ± SD, and the significance of differences between genotypes was determined by one-way ANOVA with Dunnett's multiple comparisons (*C* and *D*) or unpaired Student's *t* test (*E* and *F*) (*$P < 0.05$, **$P < 0.01$, ***$P < 0.001$, ****$P < 0.0001$).

genotype–phenotype associations pooled from multiple pedigrees, we found that damaging mutations in *Smcr8* led to increased production of TNF in response to CpG oligodeoxynucleotides, a TLR9 ligand, in two ancestrally unrelated pedigrees (R1418 and R3960) (Fig. 1 *A* and *B*). The first allele, detected in pedigree R1418, was named *patriot* and corresponded with a likely damaging missense mutation (PolyPhen-2 score = 1.0) causing an isoleucine-to-threonine substitution of the second amino acid (I2T) of the protein. The second allele, detected in pedigree R3960, was named *patriot2* and resulted in a methionine-to-valine substitution of the first amino acid (M1V), presumably destroying the translation start codon. To validate the mapping data, CRISPR/Cas9 targeting was utilized to generate mice with the I2T mutation ($Smcr8^{I2T/I2T}$) originally detected in the *patriot* pedigree, as well as a frameshift mutant with a putative null allele ($Smcr8^{-/-}$). Stimulation of peritoneal macrophages from $Smcr8^{-/-}$ and $Smcr8^{I2T/I2T}$ mice with CpG resulted in increased production of TNF compared with wild-type macrophages, validating the original linkage mapping (Fig. 1*C*).

Further investigation revealed that elevated TNF responses were also induced by activation of TLR3 with poly(I:C) or by activation of TLR7 with R848 (Fig. 1*C*). In contrast, stimulation of TLR2 with Pam_3CSK_4 or TLR4 with LPS resulted in normal levels of TNF production (Fig. 1*D*). Similar defects of IL-6 production were observed in $Smcr8^{-/-}$ bone marrow-derived dendritic cells (BMDCs), which displayed excessive IL-6 responses to poly(I:C), R848, and CpG, but normal responses to Pam_3CSK4 and LPS. (Fig. 1 *E* and *F*). These findings show that SMCR8 is necessary to limit signaling from endosomal TLRs in macrophages and myeloid dendritic cells.

Splenomegaly, Lymphadenopathy, T Cell Activation, and Elevated IL-12p40 in $Smcr8^{-/-}$ Mice. *Smcr8* CRISPR mice spontaneously exhibited signs of immune dysregulation. Splenomegaly and lymphadenopathy were observed in 9- to 12-mo-old $Smcr8^{-/-}$ and $Smcr8^{I2T/I2T}$ mice (Fig. 2 *A–D*). In the spleens of these mice, percentages of major immune cell populations including macrophages, monocytes, neutrophils, and B and T cells remained unchanged compared with wild-type mice (*SI Appendix*, Fig. S1*A*) Within the T cell compartment, we observed reduced percentages of naive ($CD3^+CD62L^+CD44^-$) and increased percentages of activated ($CD3^+CD44^+CD62L^-$) cells in both $CD4^+$ and $CD8^+$ lineages, a phenotype that was present in spleen (*SI Appendix*, Fig. S1 *B* and *C*) as well as in peripheral blood (Fig. 2 *E* and *F*). A 23plex cytokine array analysis revealed elevated plasma levels of IL-12p40 in $Smcr8^{-/-}$ and $Smcr8^{I2T/I2T}$ mice compared with control animals (Fig. 2*G* and *SI Appendix*, Fig. S1*D*). These data indicate that an overabundance of myeloid and activated lymphoid cells develop in mice lacking SMCR8 function.

Knockout of Endosomal TLR Signaling Rescues Spontaneous Inflammation. To determine whether endosomal TLR signaling contributed to the inflammatory phenotypes described above, we bred $Smcr8^{-/-}$ mice onto a $Tlr3^{-/-};Tlr7^{-/-};Tlr9^{-/-}$ ($Tlr3/7/9^{-/-}$) background. Strikingly, spleen and lymph node size were restored to normal levels in $Smcr8^{-/-};Tlr3/7/9^{-/-}$mice (Fig. 3 *A* and *B*). Hyperactivation of T cells and high circulating plasma levels of IL-12p40 observed in $Smcr8^{-/-}$ mice were also rescued to control levels on a $Tlr3/7/9^{-/-}$ background (Fig. 3 *C–E*). These data demonstrate that exaggerated signaling from one or more endosomal TLRs results in immune cell hyperplasia and T cell activation in SMCR8-deficient mice.

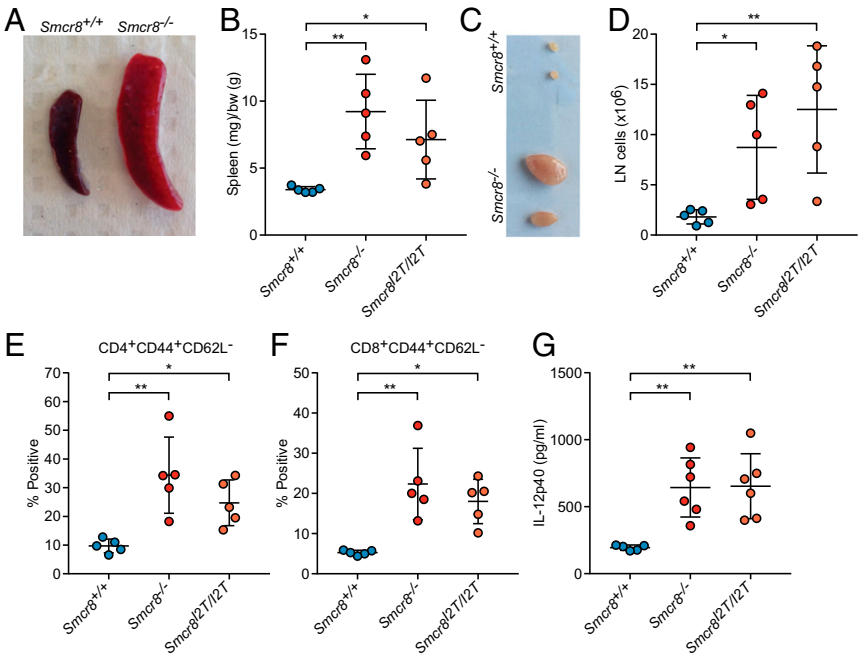

Fig. 2. Splenomegaly and lymphadenopathy in *Smcr8* mutant mice. (*A–F*) Spleens and lymph nodes were harvested from $Smcr8^{+/+}$ ($n = 5$), $Smcr8^{-/-}$ ($n = 5$), and $Smcr8^{I2T/I2T}$ ($n = 5$) mice at 12 mo of age. (*A*) Representative image of spleen harvested from $Smcr8^{-/-}$ mice. (*B*) Spleen weights normalized to body weight (bw). (*C*) Representative image and (*D*) total pooled cervical lymph node (LN) cell number harvested from two largest lymph nodes for each mouse. (*E* and *F*) Frequency of $CD44^+CD62L^-$ $CD4^+$ (*E*) and $CD8^+$ (*F*) T cells in peripheral blood. (*G*) Plasma levels of IL-12p40 detected in $Smcr8^{+/+}$ ($n = 6$), $Smcr8^{-/-}$ ($n = 6$), and $Smcr8^{I2T/I2T}$ ($n = 6$) mice at 9 mo of age. In *B*, *D*, and *E–G*, data points represent individual mice. Data are representative of three independent experiments (*A–G*). Data are expressed as means ± SD, and the significance of differences between genotypes was determined by one-way ANOVA with Dunnett's multiple comparisons (*$P < 0.05$, **$P < 0.01$).

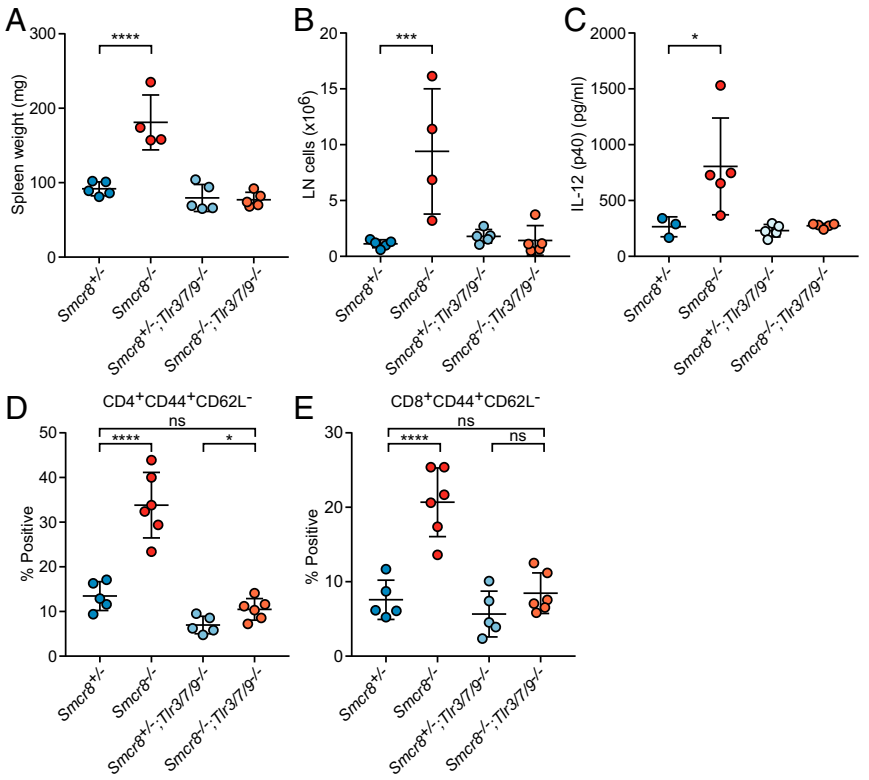

Fig. 3. Removal of TLR -3, -7, and -9 signaling rescues basal inflammation in *Smcr8*$^{-/-}$ mice. (*A* and *B*) Spleen weight (*A*) and cervical lymph node cell counts (*B*) from *Smcr8*$^{+/-}$ ($n = 5$), *Smcr8*$^{-/-}$ ($n = 4$), *Smcr8*$^{+/-}$*;Tlr3/7/9*$^{-/-}$ ($n = 5$), and *Smcr8*$^{-/-}$*Tlr3/7/9*$^{-/-}$ ($n = 5$) mice at 9 mo of age. (*C*) Plasma levels of IL-12p40 from *Smcr8*$^{+/-}$ ($n = 3$), *Smcr8*$^{-/-}$ ($n = 4$), *Smcr8*$^{+/-}$*;Tlr3/7/9*$^{-/-}$ ($n = 5$), and *Smcr8*$^{-/-}$*Tlr3/7/9*$^{-/-}$ ($n = 5$) mice at 6 mo of age. (*D* and *E*) Frequency of CD44^{+}CD62L^{-} CD4^{+} (*D*) and CD8^{+}(*E*) T cells in peripheral blood at 5 mo of age. Data points represent individual mice. Data are representative of three independent experiments. Data are expressed as means ± SD, and the significance of differences was determined by one-way ANOVA with Dunnett's multiple comparisons (ns, not significant, $P \geq 0.05$; *$P < 0.05$, ***$P < 0.001$, ****$P < 0.0001$).

SWC Complex Regulates Acidification of Cargo. TLR3, TLR7, and TLR9 engage ligands and signal from the endolysosomal compartment, a vesicular compartment formed by late endosome–lysosome fusion (20). Degradation of endocytic cargo by lysosomal hydrolases begins in endolysosomes and continues in lysosomes following maturation from endolysosomes, which involves gradually increasing acidification of the lumen. C9ORF72 reportedly localizes to lysosomes in 293T and neuronal cells (21). Moreover, we found that *Smcr8*$^{-/-}$ macrophages exhibited an accumulation of putative lysosomes (LysoTracker-positive vesicles) (Fig. 4 *A* and *B*), a phenotype also reported for C9ORF72-deficient cells (1). Considering the hyperactive TLR3/7/9 signaling in *Smcr8*$^{-/-}$ cells, this finding suggests that a block in the cycle of lysosome function might result in failure to degrade endolysosomal cargo including TLRs and their ligands, leading to prolonged ligand–receptor interaction and consequently increased signaling.

Because TLR2 and TLR4 can become incorporated and signal from phagosomes following engulfment of a particle ligand (22–24), we assessed maturation and acidification of cargo within the phagocytic pathway. We utilized pHrodo bioparticle conjugates, which exhibit a pH-dependent fluorescence that is maximal in the acidic environment of the phagolysosome. *Smcr8*$^{-/-}$ macrophages exhibited reduced mean fluorescence intensity (MFI) upon incubation with zymosan and *Escherichia coli* pHrodo BioParticles, but normal MFI after uptake of pH-insensitive BioParticles (Fig. 4 *C* and *D* and *SI Appendix*, Fig. S2), indicating normal initial uptake of cargo but impaired acidification of the phagolysosome. Slight differences ($P = 0.19$) in MFI were observed at 2 h for pH-insensitive bioparticles. Similar to the exaggerated responses to endosomal TLR ligands, *Smcr8*$^{-/-}$ BMDMs produced increased levels of TNF in response to zymosan (TLR2 ligand) and *E. coli* BioParticles (TLR4 ligand) (Fig. 4*E*). These findings support the idea that impaired vesicle acidification resulting in failure to degrade cargo in phagolysosomes leads to extended ligand–receptor contact and increased TLR signaling.

Phagosomal pH is dictated primarily by the activities of the vacuolar ATPase (V-ATPase) and NADPH oxidase (NOX2). Generation of superoxide anions by NOX2 and their subsequent dismutation into hydrogen peroxide consumes protons; thus, NOX2 activity increases the pH of the phagosome. To assess levels of reactive oxygen species (ROS) within the phagosome, zymosan particles were covalently coupled with the ROS-sensitive dye OxyBURST Green H_2DCFDA (2′,7′-dichlorodihydrofluorescein diacetate), which fluoresces brightly upon conversion to dichlorofluorescein by oxidation. Higher MFI levels were detected in *Smcr8*$^{-/-}$ macrophages after incubation with OxyBURST-zymosan, indicating that impaired acidification is at least in part caused by elevated NOX2 activity (Fig. 4*F*).

Hematopoietic Deficiency of SMCR8 Increases Sensitivity to Dextran Sodium Sulfate-Induced Colitis. In addition to screening for abnormal responses to TLR activation, G3 mutant mice were also tested for altered susceptibility to dextran sodium sulfate (DSS)-induced colitis to identify genes necessary for intestinal homeostasis (25). Mice were treated with 1.3–1.5% DSS in the drinking water for 7 d, and body weight was measured on days 0, 7, and 10 after DSS initiation. Mice homozygous for *patriot* and *patriot2* alleles were susceptible to developing colitis, losing 20% of their

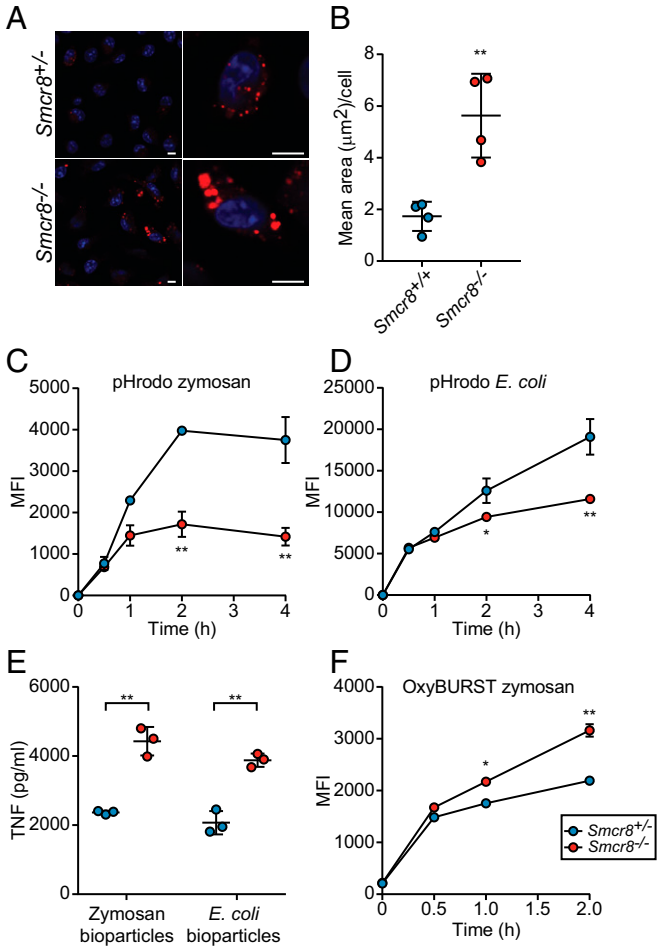

Fig. 4. Altered phagolysosomal biology in *Smcr8*$^{-/-}$ cells. (*A*) Representative images of increased LysoTracker-positive vesicles (red) in *Smcr8*$^{-/-}$ macrophages. Nuclei (blue) were stained with DAPI. (Scale bars, 5 μm.) (*B*) Quantification of LysoTracker-positive area in *Smcr8*$^{-/-}$ cells. Each data point represents the average area of LysoTracker-positive staining for independently derived cell lines ($n = 4$). A minimum of 150 cells for each cell line were utilized for quantification. (*C* and *D*) MFI of BMDMs ($n = 3$ mice per genotype) incubated for indicated times with pHrodo zymosan (*C*) or pHrodo *E. coli* BioParticles (*D*). (*E*) ELISA analysis of TNF secretion by BMDMs ($n = 3$ mice per genotype) stimulated for 6 h with 10 μg/mL zymosan or *E. coli* BioParticles. (*F*) MFI of BMDMs ($n = 3$ mice per genotype) incubated for indicated times with OxyBURST zymosan. Data are representative of three independent experiments. In *B* and *E*, data points represent individual mice. Data are expressed as means ± SD, and the significance of differences between genotypes was determined by unpaired Student's *t* test (*B*–*E*) (*$P < 0.05$, **$P < 0.01$).

initial body weight by days 7 and 10 of the treatment, respectively (Fig. 5 *A*–*D*), whereas wild-type mice lost an average of 5% of their initial body weight. Consistent with the mapping data, *Smcr8*$^{-/-}$ and *Smcr8*$^{I2T/I2T}$ mice also displayed increased susceptibility to DSS treatment compared with wild-type controls, exhibiting 20% weight loss by day 8 (Fig. 5*E*). Compared with wild-type mice, both CRISPR lines exhibited an elevated disease activity index (DAI) including weight loss, severe diarrhea, intestinal bleeding, and colonic shortening (Fig. 5 *F* and *G*). Histopathological alterations characterized by infiltrating leukocytes and loss of crypt architecture were also apparent in *Smcr8*$^{-/-}$ and *Smcr8*$^{I2T/I2T}$ mice but not in wild-type mice (*SI Appendix*, Fig. S3).

To test the dependence of the DSS-induced colitis phenotype on cells of the hematopoietic compartment, we generated bone marrow chimeras. Wild-type mice reconstituted with *Smcr8*$^{-/-}$ bone marrow exhibited increased body weight loss and DAI compared with those reconstituted with wild-type bone marrow, suggesting that SMCR8 functions in hematopoietic cells to protect against DSS-induced colitis (Fig. 5 *H* and *I*). To determine if exaggerated endosomal TLR signaling was responsible for the colitis susceptibility conferred by *Smcr8*$^{-/-}$ hematopoietic cells, we reconstituted lethally irradiated wild-type mice with bone marrow from *Smcr8*$^{+/-}$, *Smcr8*$^{-/-}$, *Smcr8*$^{+/-}$;*Tlr3/7/9*$^{-/-}$, or *Smcr8*$^{-/-}$;*Tlr3/7/9*$^{-/-}$ mice and treated them with DSS to induce colitis. Recipients of *Smcr8*$^{-/-}$ bone marrow showed weight losses similar to recipients of *Smcr8*$^{-/-}$;*Tlr3/7/9*$^{-/-}$ bone marrow on day 10 of the DSS treatment protocol. Thus, although elevated susceptibility to DSS-induced colitis can be attributed to hematopoietic deficiency of SMCR8, knockout of endosomal TLR signaling does not rescue this phenotype (Fig. 5*J*).

***Wdr41* Mutant Mice Phenocopy *Smcr8* Mutant Mice.** While screening ENU-mutagenized mice for hematopoietic alterations in peripheral blood, we detected an increase in CD44^{+}CD62L^{-} T cells in mice homozygous mice for a splice donor site mutation in *Wdr41* (Fig. 6 *A* and *B*). The phenotype was named *gogi*. The *gogi* allele was also associated with increased DSS-induced colitis susceptibility with homozygotes losing 20% of their body weight by day 8 (Fig. 6*C*). *Wdr41*$^{gogi/gogi}$ mice displayed elevated plasma levels of IL-12p40 under basal conditions without DSS treatment (Fig. 6*D*). Stimulation of peritoneal macrophages harvested from *Wdr41*$^{gogi/gogi}$ mice with poly(I:C), R848, and CpG resulted in increased TNF production (Fig. 6*E*). A second allele resulting in a premature stop codon in *Wdr41* was also generated during ENU mutagenesis. Peritoneal macrophages homozygous for this allele, *metallica* (*mca*), were hyperresponsive to endosomal TLR ligands (*SI Appendix*, Fig. S4*A*), and *Wdr41*$^{mca/mca}$ mice exhibited increased frequencies of activated T cells in the peripheral blood (*SI Appendix*, Fig. S4 *B* and *C*).

Discussion

Here, we have established that exaggerated TLR signaling is elicited in myeloid cells from *Smcr8*$^{-/-}$ and *Smcr8*$^{I2T/I2T}$ mice by ligands normally encountered in endolysosomes and that such signaling in cell type(s) yet to be identified drives the spontaneous inflammation observed in *Smcr8*$^{-/-}$ mice. Secondary lymphoid organ enlargement, activation of T cells, and elevated IL-12p40 serum levels were rescued by ablation of endosomal TLR signaling. We note that the source of ligand (i.e., microbial vs. sterile) responsible for the spontaneous inflammation in *Smcr8*$^{-/-}$ mice remains unknown, as does the identity of the cell type that primarily drives the immune dysregulation. Cell-specific targeting of *Smcr8* in myeloid and lymphoid lineages will aid in determining the roles that each cell population plays in the observed phenotypes. In addition, the contribution of individual TLRs to the inflammatory phenotypes warrants further investigation.

While the requirement of endolysosomal acidification for TLR3, TLR7, and TLR9 activation is well known (26–29), our data instead show increased TLR signaling despite impaired acidification, at least in phagolysosomes. We conclude that the level of acidification of phagolysosomes in *Smcr8*$^{-/-}$ cells is sufficient for TLR activation, but perhaps inadequate for optimal function of the hydrolases responsible for degradation of phagocytosed TLR ligands. This idea is supported by the observation of lysosome accumulation in *Smcr8*$^{-/-}$ macrophages because lysosome turnover requires degradation and removal of degraded cargo via diffusion or specific transport (20, 30). Our data thus suggest a critical role for SMCR8, and likely for the SWC complex itself, that occurs after late endosome or phagosome fusion with the lysosomal compartment in the membrane trafficking cycle. One possibility suggested by the elevated phagosomal ROS levels observed in *Smcr8*$^{-/-}$ macrophages is that the SWC complex negatively regulates recruitment of

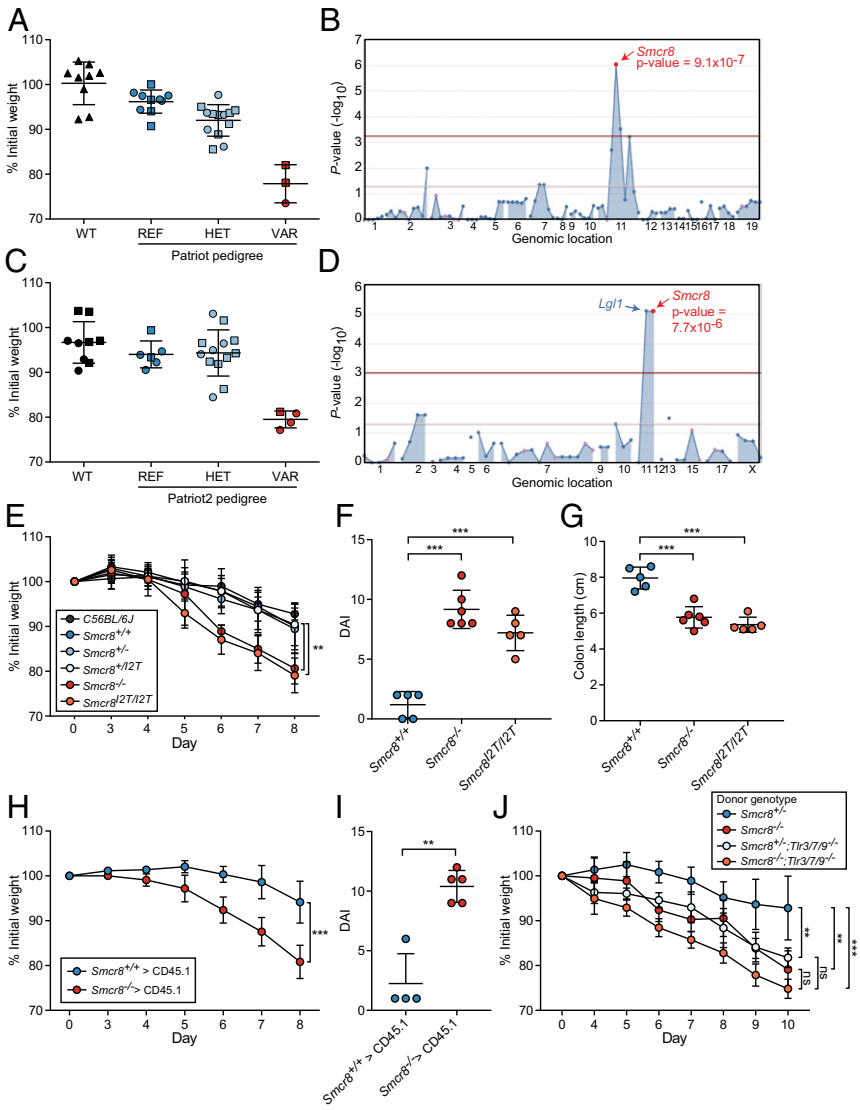

Fig. 5. Mapping and validation of colitis phenotype caused by *Smcr8* mutations. (*A* and *C*) Weight loss analysis of *patriot* mice (*A*) on day 7 of DSS treatment [REF, $Smcr8^{+/+}$ ($n = 10$); HET, $Smcr8^{+/p}$ ($n = 13$); VAR, $Smcr8^{p/p}$ ($n = 3$)], and *patriot2* mice (*C*) on day 10 of DSS treatment [REF, $Smcr8^{+/+}$ ($n = 6$); HET, $Smcr8^{+/p2}$ ($n = 13$); VAR, $Smcr8^{p2/p2}$ ($n = 4$)]. (*B* and *D*) Manhattan plots showing *P* values of association between the *patriot* phenotype (*B*) and the *patriot2* phenotype (*D*) and mutations identified in the pedigrees in *A* and *C*, respectively, calculated using a recessive model of inheritance. The $-\log_{10}$ *P* values were plotted versus the chromosomal positions of mutations. Horizontal red and purple lines represent thresholds of $P = 0.05$ with or without Bonferroni correction, respectively. (*E*) Weight loss analysis of $Smcr8^{+/+}$ ($n = 6$), $Smcr8^{+/-}$ ($n = 7$), $Smcr8^{+/I2T}$ ($n = 7$), $Smcr8^{-/-}$ ($n = 7$), and $Smcr8^{I2T/I2T}$ ($n = 7$) mice treated with 1.4% DSS. (*F*) DAI and (*G*) colon length (cm) of $Smcr8^{+/+}$ ($n = 5$), $Smcr8^{-/-}$ ($n = 6$), and $Smcr8^{I2T/I2T}$ ($n = 5$) mice after 7 d of 1.4% DSS treatment. (*H* and *I*) Wild-type mice were lethally irradiated and reconstituted with $Smcr8^{+/+}$ ($n = 4$) or $Smcr8^{-/-}$ ($n = 5$) bone marrow. Weight loss analysis (*H*) on the indicated days of treatment and DAI (*I*) after 7 d of treatment with 1.4% DSS. (*J*) Wild-type mice were lethally irradiated and reconstituted with bone marrow of the indicated donor genotype. Weight loss analysis of recipient mice treated with 1.4% DSS ($n = 5$ for all groups). Data are representative of one experiment (*A–D*) or three independent experiments (*E–J*). In *A*, *C*, *F*, *G*, and *I*, data points represent individual mice. Data are expressed as means ± SD, and the significance of differences between genotypes was determined by one-way ANOVA with Dunnett's multiple comparisons (*E–G* and *J*) or unpaired Student's *t* test (*H* and *I*) (ns, not significant, $P \geq 0.05$; $^{**}P < 0.01$, $^{***}P < 0.001$, $^{****}P < 0.0001$). For *E*, *H*, and *J*, the statistical assessment for the last time point is indicated.

NOX2 to phagolysosomes and endolysosomes; this may be achieved through modulation of Rab activity, which has been shown to regulate NOX2 recruitment to phagosomes in dendritic cells (31). As a consequence of impaired degradation of lysosomal cargo including TLR3, TLR7, TLR9, and/or their ligands, prolonged ligand–receptor interactions result in correspondingly prolonged signaling.

The proposed model for negative regulation of endosomal TLR signaling by the SWC complex provides a plausible mechanistic explanation for the autoimmune phenotypes observed in $C9orf72^{-/-}$ and $Smcr8^{-/-}$ mice. Effective and timely degradation of phagocytosed dead cells by macrophages precludes macrophage activation by nucleic acids released from dying cells and presentation of self peptides to T cells. However, in $Smcr8^{-/-}$ macrophages degradation of such cargo may be both delayed and impaired, resulting in preservation of nucleic acids and peptides presented to T cells and subsequent development of cellular and humoral immunity against self DNA and autoantigens. In humans with ALS/FTD caused by C9ORF72 mutations, it may be that such autoantigens include nervous system proteins important for motor neuron function.

Loss of SMCR8 function in hematopoietic cells also rendered mice susceptible to chemically induced colitis. Removal of signaling through TLRs -3, -7, and -9 in hematopoietic cells did not

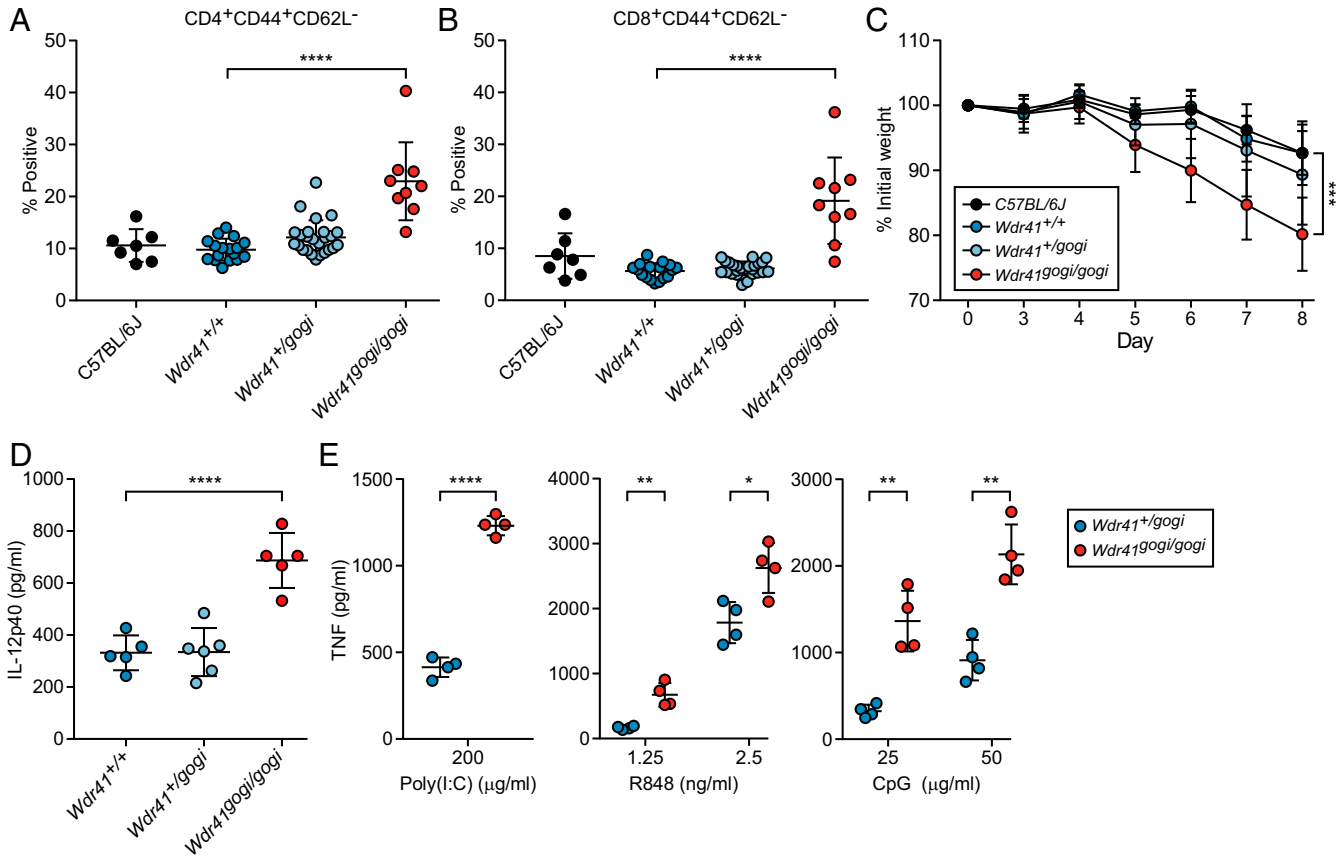

Fig. 6. WDR41 deficiency phenocopies loss of SMCR8 function. (*A* and *B*) Frequency of $CD44^+CD62L^-$ $CD4^+$ (*A*) and $CD8^+$ (*B*) T cells in peripheral blood from C57BL/6J mice ($n = 7$) and G3 mice from a single pedigree carrying the $Wdr41^{gogi}$ allele [$Wdr41^{+/+}$ ($n = 17$), $Wdr41^{+/gogi}$ ($n = 25$), and $Wdr41^{gogi/gogi}$ ($n = 9$)]. (*C*) Weight loss analysis of C57BL/6J ($n = 10$), $Wdr41^{+/+}$ ($n = 7$), $Wdr41^{+/gogi}$ ($n = 14$), and $Wdr41^{gogi/gogi}$ ($n = 6$) treated with 1.4% DSS. (*D*) Plasma levels of IL-12p40 detected in untreated 6-mo-old *gogi* mice [$Wdr41^{+/+}$ ($n = 5$), $Wdr41^{+/gogi}$ ($n = 5$), and $Wdr41^{gogi/gogi}$ ($n = 5$)]. (*E*) ELISA analysis of TNF secretion by peritoneal macrophages ($n = 4$ mice per genotype) stimulated for 6 h with indicated concentrations of poly(I:C), R848, and CpG. In *A*, *B*, *D*, and *E*, data points represent individual mice. Data are representative of two independent experiments. Data are expressed as means ± SD, and the significance of differences between genotypes was determined by one-way ANOVA with Dunnett's multiple comparisons (*A*–*D*) or unpaired Student's *t* test (*E*) (*$P < 0.05$, **$P < 0.01$, ***$P < 0.001$, ****$P < 0.0001$). For *C*, the statistical assessment for the last time point is indicated.

rescue colitis susceptibility observed in $Smcr8^{-/-}$ mice and perhaps worsened disease. Moreover, mice reconstituted with $Smcr8^{+/-}$;$Tlr3/7/9^{-/-}$ bone marrow were more susceptible compared with mice reconstituted with $Smcr8^{+/-}$ bone marrow. These findings are consistent with reports of the requirement for endosomal TLR receptors in protection from colitis (32–34). Activation of these receptors appears to be important for reducing inflammation during DSS-induced colitis (TLR3 and TLR7) and for epithelial restitution during wound repair (TLR9) (33, 34). While complete ablation of endosomal TLR responses appears to increase sensitivity to DSS, the possibility remains that hyperactivation of these receptors also increases susceptibility and is contributory to the DSS phenotype observed in $Smcr8^{-/-}$ mice. With that said, $Smcr8^{-/-}Tlr3/7/9^{-/-}$ chimeric mice showed a trend towards more body weight loss than $Smcr8^{+/-}$;$Tlr3/7/9^{-/-}$ chimeric mice after DSS challenge ($P = 0.14$), suggesting the presence of defects independent of endosomal TLR signaling. DSS insult physically compromises the intestinal epithelial barrier allowing for the entry of luminal microbes that must be cleared for restoration of intestinal homeostasis. We hypothesize that challenge of *Smcr8* CRISPR mice with DSS may result in the hyperactivation of pathogenic immune signaling responses associated with endosomes and phagosomes after internalization of these microbes. Moreover, $Smcr8^{-/-}$ macrophages exhibited increased production of phagosomal ROS, which has been shown to contribute to disease severity in DSS colitis (35, 36).

Spontaneous inflammation has been reported in mice with C9ORF72 or SMCR8 deficiency, but loss of function of the third SWC complex member, WDR41, has not been examined. We showed that mice homozygous for damaging mutations in *Wdr41* phenocopied $Smcr8^{-/-}$ mice in hyperactivation of T cells and elevated serum IL-12p40 levels under basal conditions, as well as colitis susceptibility after DSS challenge. Taken together, all members of the tripartite complex appear to be necessary for immune regulation.

Materials and Methods

Mice. Eight- to 10-wk-old C57BL/6J mice were purchased from The Jackson Laboratory. ENU mutagenesis was performed as previously described (37). Briefly, mutagenized G0 males were bred to C57BL/6J females, and the resulting G1 males were crossed to C57BL/6J females to produce G2 mice. G2 females were backcrossed to their G1 sires to yield G3 mice, which were screened for phenotypes. Whole-exome sequencing and mapping were performed as described previously (38).

For the DSS-induced colitis screen, mice received 1.3–1.5% DSS in the drinking water for 7 d followed by an additional 3 d off DSS. Weight was recorded daily and reported as a percentage relative to the pretreatment weight. Briefly, DAI was scored cumulatively as follows: weight loss—0 (no loss), 1 (1–10% loss of body weight), 2 (10–15% loss of body weight), 3 (15–20% loss of body weight), and 4 (>20% loss of body weight); stool consistency—0 (normal), 2 (loose stool), and 4 (diarrhea); and bleeding—0

(no blood), 1 (hemoccult-positive), 2 (hemoccult-positive and visual pellet bleeding), and 4 (gross bleeding and/or blood around anus).

Smcr8$^{-/-}$; *Tlr3*$^{-/-}$; *Tlr7*$^{-/-}$;*Tlr9*$^{-/-}$ mice were generated by intercrossing single knockout mouse strains. The *Tlr3*$^{-/-}$ (39), *Tlr7*$^{-/-}$ (40), and *Tlr9*$^{-/-}$ (41) mutant mice have been previously described. All mice were housed in the University of Texas Southwestern vivarium. All procedures were approved by the University of Texas Southwestern Medical Center Institutional Animal Care and Use Committee, and performed in accordance with institutionally approved protocols.

Generation of the Smcr8$^{I2T/I2T}$ and Smcr8$^{-/-}$ Mouse Strains Using the CRISPR/Cas9 System. To generate *Smcr8*$^{I2T/I2T}$ and *Smcr8*$^{-/-}$ mouse strains, female C57BL/6J mice were superovulated by injection of 6.5 U pregnant mare serum gonadotropin (Millipore), followed by injection of 6.5 U human chorionic gonadotropin (Sigma-Aldrich) 48 h later. The superovulated mice were subsequently mated overnight with C57BL/6J male mice. The following day, fertilized eggs were collected from the oviducts, and in vitro-transcribed Cas9 mRNA (50 ng/μL) and Smcr8 small base-pairing guide RNA (50 ng/μL; 5′-GGGATCTTCGTCTTCTGACG-3′ for *Smcr8*$^{-/-}$ and 5′-GATCAGCGCCCCTGATGTGG-3′ for *Smcr8*$^{I2T/I2T}$ mice) were injected into the cytoplasm or pronucleus of the embryos. The injected embryos were cultured in M16 medium (Sigma-Aldrich) at 37 °C in 5% CO_2. For the production of mutant mice, two-cell-stage embryos were transferred into the ampulla of the oviduct (10–20 embryos per oviduct) of pseudopregnant Hsd:ICR (CD-1) female mice (Harlan Laboratories).

Smcr8$^{-/-}$ mice contain a 26-bp deletion of chromosome 11 (60,778,048–60,778,073) in exon 1, resulting in a predicted frameshifted protein product beginning after amino acid 7 of the protein and terminating after the inclusion of six aberrant amino acids. *Smcr8*$^{I2T/I2T}$ mice contain three separate point mutations on chromosome 11: 60,778,032 (T→C), 60,778,048 (G→A), and 60,778,078 (G→A). The first mutation results in an isoleucine-to-threonine change in amino acid 2 of the protein while the latter two are silent and result in no coding changes.

Hematopoietic Chimeras. The indicated recipient mice were irradiated with two doses of 6.5 Gy spaced 4 h apart. Bone marrow cells from the tibiae and femurs of donors were i.v. injected into recipients. Mice were maintained for 2 wk on water containing trimethroprim–sulfamethoxazole antibiotics, and experiments were performed 8–10 wk after reconstitution.

Peritoneal Macrophage, BMDC, and BMDM Cultures. Peritoneal macrophages were isolated as previously described (42). Mice were injected intraperitoneally with Brewer's modified thioglycolate (3% wt/vol; BD Biosciences). Cells were collected by peritoneal lavage with 5 mL of PBS on day 5 after injection, plated onto 96-well plates at a density of 1×10^5 cells/well overnight, and stimulated with the indicated ligands. Cells were subjected to MTT assay (Sigma-Aldrich) for normalization.

BMDCs and BMDMs were generated by standard protocols. Briefly, bone marrow was isolated from femurs and tibias of mice. Bone marrow cells were cultured in recombinant GM-CSF (33 ng/mL) or M-CSF (20 ng/mL) for 6 d. BMDCs were plated onto 96-well plates at a density of 1×10^5 cells/well and stimulated with the indicated ligands. BMDMs were plated onto 24-well plates at a density of 5×10^5 cells/well for microbial BioParticle uptake and response experiments.

Antibodies and Reagents. The following antibodies were used: B220, CD3, CD4, CD11c, CD19, CD44, Ly-6G (BD Biosciences), CD8, CD11b, CD86, Ly-6C, (BioLegend), and CD62L, F4/80 (Tonbo Biosciences).

The following reagents were used: Pam3CSK4 and R848 (InvivoGen); poly (I:C) (GE Healthcare); LPS and MALP-2 (Enzo Life Sciences); CpG-ODN 1668 (Sigma-Aldrich); and mouse IL-6, IL-12p40, and TNF-α Ready-SET-Go kits (eBioscience).

Flow Cytometry. Spleen and blood cells were isolated and incubated as previously described (38). Data were acquired on a LSR II Fortessa cell analyzer (BD Biosciences) and analyzed with FlowJo software (FlowJo). Cell sorting was performed on a FACSAria II cell sorter (BD Biosciences).

Microscopy. BMDMs were plated onto eight-well glass bottom μ-slides (ibidi) at a density of 2×10^5 cells/well. Cells were incubated with 300 nM LysoTracker for 15 min for visualization of lysosomes. Images were acquired using 63× objectives of a Zeiss LSM880 inverted confocal microscope.

Histology. Freshly isolated distal colons were fixed in formalin and embedded in paraffin. Hematoxylin/eosin staining was conducted using a standard protocol by the University of Texas Southwestern Histology core.

Statistical Analysis. The statistical significance of differences between groups was analyzed using GraphPad Prism software. Data are expressed as means ± SD, and significance was determined by one-way ANOVA with Dunnett's multiple comparisons or unpaired Student's *t* test. Differences with P values ≥ 0.05 were considered to be not significant (ns). All differences with P values < 0.05 were considered significant. P values are denoted by $^*P < 0.05$, $^{**}P < 0.01$, $^{***}P < 0.001$, and $^{****}P < 0.0001$.

ACKNOWLEDGMENTS. This work was supported by Crohn's and Colitis Foundation Fellowship Award 2014CCFA00RFA0000090037 (to E.T.); Immunology T32 Training Grant AI005184 at UT Southwestern Medical Center (to W.M.); NIH Grants K08 DK107886 (to E.T.), R37 GM066759 (to B.B.), R01 AI125581 (to B.B.), and U19 AI100627 (to B.B.); and by the Lyda Hill Foundation.

1. O'Rourke JG, et al. (2016) C9orf72 is required for proper macrophage and microglial function in mice. *Science* 351:1324–1329.
2. Sullivan PM, et al. (2016) The ALS/FTLD associated protein C9orf72 associates with SMCR8 and WDR41 to regulate the autophagy-lysosome pathway. *Acta Neuropathol Commun* 4:51.
3. Yang M, et al. (2016) A C9ORF72/SMCR8-containing complex regulates ULK1 and plays a dual role in autophagy. *Sci Adv* 2:e1601167.
4. Ugolino J, et al. (2016) Loss of C9orf72 enhances autophagic activity via deregulated mTOR and TFEB signaling. *PLoS Genet* 12:e1006443.
5. Jung J, et al. (2017) Multiplex image-based autophagy RNAi screening identifies SMCR8 as ULK1 kinase activity and gene expression regulator. *eLife* 6:e23063.
6. Webster CP, et al. (2016) The C9orf72 protein interacts with Rab1a and the ULK1 complex to regulate initiation of autophagy. *EMBO J* 35:1656–1676.
7. Farg MA, et al. (2014) C9ORF72, implicated in amytrophic lateral sclerosis and frontotemporal dementia, regulates endosomal trafficking. *Hum Mol Genet* 23: 3579–3595.
8. Sellier C, et al. (2016) Loss of C9ORF72 impairs autophagy and synergizes with polyQ Ataxin-2 to induce motor neuron dysfunction and cell death. *EMBO J* 35:1276–1297.
9. Zhang D, Iyer LM, He F, Aravind L (2012) Discovery of novel DENN proteins: Implications for the evolution of eukaryotic intracellular membrane structures and human disease. *Front Genet* 3:283.
10. Levine TP, Daniels RD, Gatta AT, Wong LH, Hayes MJ (2013) The product of C9orf72, a gene strongly implicated in neurodegeneration, is structurally related to DENN Rab-GEFs. *Bioinformatics* 29:499–503.
11. DeJesus-Hernandez M, et al. (2011) Expanded GGGGCC hexanucleotide repeat in noncoding region of C9ORF72 causes chromosome 9p-linked FTD and ALS. *Neuron* 72: 245–256.
12. Turner MR, Goldacre R, Ramagopalan S, Talbot K, Goldacre MJ (2013) Autoimmune disease preceding amyotrophic lateral sclerosis: An epidemiologic study. *Neurology* 81:1222–1225.
13. Miller ZA, et al. (2016) Increased prevalence of autoimmune disease within C9 and FTD/MND cohorts: Completing the picture. *Neurol Neuroimmunol Neuroinflamm* 3: e301.
14. de Pasqua S, et al. (2017) Amyotrophic lateral sclerosis and myasthenia gravis: Association or chance occurrence? *Neurol Sci* 38:441–444.
15. Gotaas HT, Skeie GO, Gilhus NE (2016) Myasthenia gravis and amyotrophic lateral sclerosis: A pathogenic overlap. *Neuromuscul Disord* 26:337–341.
16. Burberry A, et al. (2016) Loss-of-function mutations in the C9ORF72 mouse ortholog cause fatal autoimmune disease. *Sci Transl Med* 8:347ra93.
17. Atanasio A, et al. (2016) C9orf72 ablation causes immune dysregulation characterized by leukocyte expansion, autoantibody production, and glomerulonephropathy in mice. *Sci Rep* 6:23204.
18. Zhang Y, et al. (2018) The C9orf72-interacting protein Smcr8 is a negative regulator of autoimmunity and lysosomal exocytosis. *Genes Dev* 32:929–943.
19. Blasius AL, Beutler B (2010) Intracellular toll-like receptors. *Immunity* 32:305–315.
20. Huotari J, Helenius A (2011) Endosome maturation. *EMBO J* 30:3481–3500.
21. Amick J, Roczniak-Ferguson A, Ferguson SM (2016) C9orf72 binds SMCR8, localizes to lysosomes, and regulates mTORC1 signaling. *Mol Biol Cell* 27:3040–3051.
22. Underhill DM, et al. (1999) The Toll-like receptor 2 is recruited to macrophage phagosomes and discriminates between pathogens. *Nature* 401:811–815.
23. Pauwels AM, Trost M, Beyaert R, Hoffmann E (2017) Patterns, receptors, and signals: Regulation of phagosome maturation. *Trends Immunol* 38:407–422.
24. Wang Y, et al. (2007) Lysosome-associated small Rab GTPase Rab7b negatively regulates TLR4 signaling in macrophages by promoting lysosomal degradation of TLR4. *Blood* 110:962–971.
25. Turer E, et al. (2017) Creatine maintains intestinal homeostasis and protects against colitis. *Proc Natl Acad Sci USA* 114:E1273–E1281.
26. Häcker H, et al. (1998) CpG-DNA-specific activation of antigen-presenting cells requires stress kinase activity and is preceded by non-specific endocytosis and endosomal maturation. *EMBO J* 17:6230–6240.
27. Park B, et al. (2008) Proteolytic cleavage in an endolysosomal compartment is required for activation of toll-like receptor 9. *Nat Immunol* 9:1407–1414.

28. Ewald SE, et al. (2008) The ectodomain of toll-like receptor 9 is cleaved to generate a functional receptor. *Nature* 456:658–662.
29. Ewald SE, et al. (2011) Nucleic acid recognition by toll-like receptors is coupled to stepwise processing by cathepsins and asparagine endopeptidase. *J Exp Med* 208: 643–651.
30. Schulze H, Kolter T, Sandhoff K (2009) Principles of lysosomal membrane degradation: Cellular topology and biochemistry of lysosomal lipid degradation. *Biochim Biophys Acta* 1793:674–683.
31. Jancic C, et al. (2007) Rab27a regulates phagosomal pH and NADPH oxidase recruitment to dendritic cell phagosomes. *Nat Cell Biol* 9:367–378.
32. Vijay-Kumar M, et al. (2007) Activation of toll-like receptor 3 protects against DSS-induced acute colitis. *Inflamm Bowel Dis* 13:856–864.
33. Rose WA, II, Sakamoto K, Leifer CA (2012) TLR9 is important for protection against intestinal damage and for intestinal repair. *Sci Rep* 2:574.
34. Yang JY, et al. (2016) Enteric viruses ameliorate gut inflammation via toll-like receptor 3 and toll-like receptor 7-mediated interferon-β production. *Immunity* 44: 889–900.
35. You Y, Fu JJ, Meng J, Huang GD, Liu YH (2009) Effect of N-acetylcysteine on the murine model of colitis induced by dextran sodium sulfate through up-regulating PON1 activity. *Dig Dis Sci* 54:1643–1650.
36. Li B, Alli R, Vogel P, Geiger TL (2014) IL-10 modulates DSS-induced colitis through a macrophage-ROS-NO axis. *Mucosal Immunol* 7:869–878.
37. Georgel P, Du X, Hoebe K, Beutler B (2008) ENU mutagenesis in mice. *Methods Mol Biol* 415:1–16.
38. Wang T, et al. (2015) Real-time resolution of point mutations that cause phenovariance in mice. *Proc Natl Acad Sci USA* 112:E440–E449.
39. Alexopoulou L, Holt AC, Medzhitov R, Flavell RA (2001) Recognition of double-stranded RNA and activation of NF-kappaB by toll-like receptor 3. *Nature* 413: 732–738.
40. Hemmi H, et al. (2002) Small anti-viral compounds activate immune cells via the TLR7 MyD88-dependent signaling pathway. *Nat Immunol* 3:196–200.
41. Hemmi H, et al. (2000) A toll-like receptor recognizes bacterial DNA. *Nature* 408: 740–745.
42. Sun L, et al. (2017) HCFC2 is needed for IRF1- and IRF2-dependent *Tlr3* transcription and for survival during viral infections. *J Exp Med* 214:3263–3277.